Identification of larvae of three arctic species of Limanda *(Family Pleuronectidae)*

Morgan S. Busby, Deborah M. Blood & Ann C. Matarese

Polar Biology

ISSN 0722-4060

Polar Biol
DOI 10.1007/s00300-017-2153-9

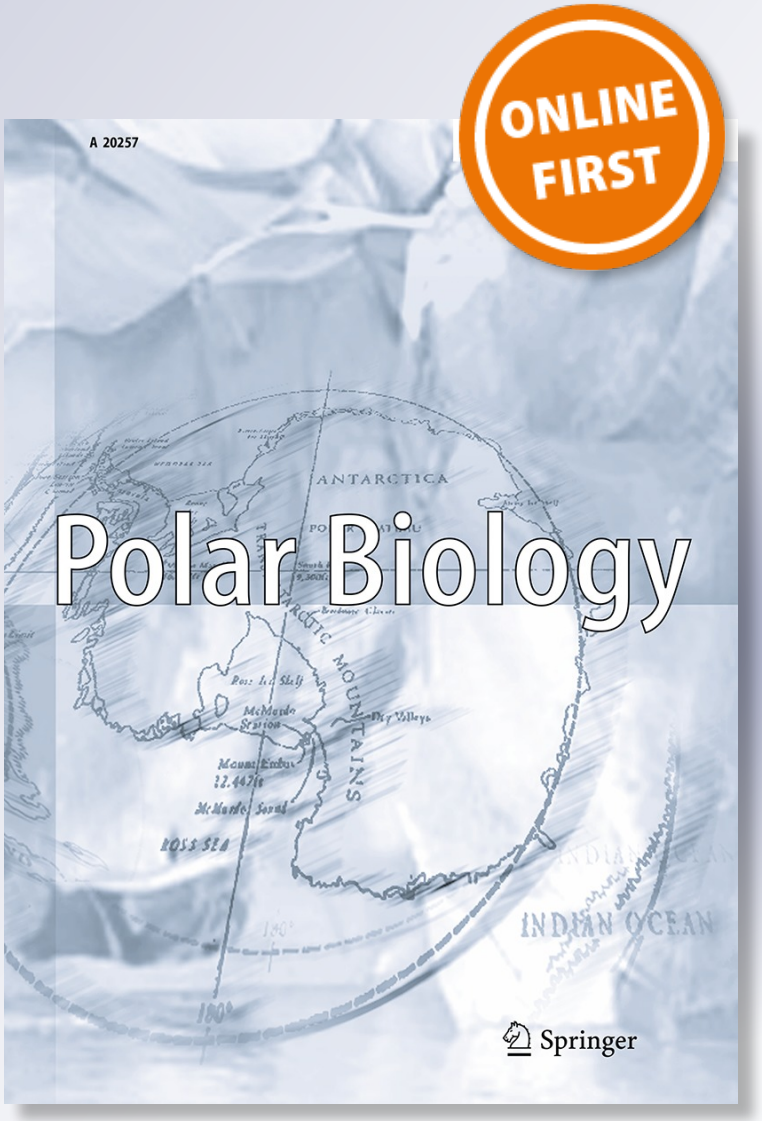

Springer

Polar Biol
DOI 10.1007/s00300-017-2153-9

ORIGINAL PAPER

Identification of larvae of three arctic species of *Limanda* (Family Pleuronectidae)

Morgan S. Busby[1] · Deborah M. Blood[1] · Ann C. Matarese[1]

Received: 28 September 2016 / Revised: 26 June 2017 / Accepted: 27 June 2017

Abstract Identification of fish larvae in Arctic marine waters is problematic as descriptions of early-life-history stages exist for few species. Our goal in this study is to provide descriptions that enable researchers to distinguish larvae of righteye flounders (family Pleuronectidae) of the genus *Limanda* that are among the most abundant fishes and frequently collected pleuronectid larvae in the northern Bering, Chukchi, and Beaufort seas. Three species of *Limanda* are represented: *L. aspera* (yellowfin sole), *L. proboscidea* (longhead dab), and *L. sakhalinensis* (Sakhalin sole). Partial descriptions of *L. aspera* and *L. proboscidea* larvae have been previously published, but content and illustrations are inadequate for making positive identifications; therefore, each species is redescribed here with updated illustrations. Larvae of *L. sakhalinensis* are described for the first time. Descriptions of meristic, morphometric, and pigment characteristics with species comparisons of larvae are presented. Primary characters that distinguish the three species are pigmentation, body depth, and length of larvae and early juveniles at developmental stage landmarks. Pigment characters during the early and late larval stages of *L. proboscidea* and its large size at transformation are different compared to *L. aspera* and *L. sakhalinensis*. These disparate larval characters described for *L. proboscidea* in comparison to the other two species provide additional evidence suggesting the genus *Limanda* may be paraphyletic, as has been proposed in other studies. Results presented here have potential utility in future Arctic fisheries oceanography research.

Keywords Arctic · Ichthyoplankton · Chukchi Sea · Pleuronectidae · Genus *Limanda*

Introduction

Interest in biological communities in Arctic ecosystems has grown dramatically as the result of rapid loss of sea-ice, increased potential for oil and gas development, and expanded transportation routes. A goal of several programs including the Arctic Ecosystem Integrated Survey (Arctic Eis); Chukchi Acoustics, Oceanography, and Zooplankton Study (CHAOZ); and Russian-American Long-Term Census of the Arctic (RUSALCA) is to assess the abundance and distribution of ichthyo- and zooplankton in Arctic ecosystems. Central to the success of these programs is the ability to identify organisms at all life stages. Identification of all fish species throughout development is necessary for baseline assessments of population structure and abundance and to understand life history processes and potential vulnerabilities.

The Recruitment Processes Program at the Alaska Fisheries Science Center (AFSC) conducts ongoing studies on identification of early-life stages of fish found in Arctic waters. The most current estimate of the number of fish taxa inhabiting Arctic waters is 242 species, distributed among 45 families (Mecklenburg et al. 2011). Of these, larvae of about 30 species, mostly from the Pacific Arctic region, can be identified (roughly 12%, AFSC unpubl.

Electronic supplementary material The online version of this article (doi:10.1007/s00300-017-2153-9) contains supplementary material, which is available to authorized users.

✉ Morgan S. Busby
morgan.busby@noaa.gov

[1] Recruitment Processes Program, Resource Assessment and Conservation Engineering Division, Alaska Fisheries Science Center, NOAA, National Marine Fisheries Service, 7600 Sand Point Way NE, Seattle, WA 98115, USA

Published online: 26 July 2017

data). Ten species of pleuronectids are present in the Arctic Ocean Basin and adjacent boreal waters (Mecklenburg et al. 2011). Fishes of the genus *Limanda* are the most frequently collected pleuronectid larvae in the northern Bering, Chukchi, and Beaufort seas and among the most abundant adult fishes. Three species are collected: *Limanda aspera* (yellowfin sole), *L. proboscidea* (longhead dab), and *L. sakhalinensis* (Sakhalin sole). Larvae of *Limanda aspera* collected during the 2004 RUSALCA ichthyoplankton survey in the Chukchi Sea were second in abundance (Norcross et al. 2010) and were the most abundant larvae overall in all Chukchi Sea ichthyoplankton surveys 2007–2011 (Logerwell et al. 2015).

Adult *L. aspera* range from the Beaufort Sea off Point Barrow (and possibly farther east) south to Atka Island in the Aleutian Archipelago and Gulf of Alaska to San Juan Island, Puget Sound, Washington, and the Sea of Japan off Korea (Mecklenburg et al. 2002; Pietsch and Orr 2015). *Limanda proboscidea* adults have been reported from the Beaufort Sea off Point Barrow to the eastern Bering Sea north of Unimak Island and to the Sea of Okhotsk (Mecklenburg et al. 2002; Logerwell et al. 2015) and *L. sakhalinensis* occur from the Chukchi and southeastern Bering seas to the Sea of Okhotsk and Tartar Strait (Mecklenburg et al. 2002). Our study area, the northern Bering and Chukchi seas, are vast continental shelf ecosystems connecting western Alaska and the Russian Far-East (Siberia), with depths typically less than 100 m and extensive portions less than 50 m (Fig. 1). In the northern Bering and Chukchi seas, all three species are typically encountered at depths less than 100 m.

Early-life-history stages of *L. aspera* and *L. proboscidea* were partially described by Pertseva-Ostroumova (1961) and Grigor'ev (2004). However, the illustrations of *L. aspera* by Pertseva-Ostroumova (1961) were of poor reproduction quality and questionable accuracy, and descriptions of *L. proboscidea* by Grigor'ev (2004) were incomplete, only covering preflexion and early-flexion stages. In this study, we describe the development of larvae of all three species from preflexion to postflexion stage (and transformation stage, when available) and provide characters and updated illustrations to distinguish the three species from each other and from other Arctic pleuronectids. Taxonomic descriptions of meristic, morphological, and melanistic pigmentation characters and ossification sequence of bony structures are presented.

This work is of substantial importance as *L. aspera* in the eastern Bering Sea supports the largest flatfish fishery in the United States (Wilderbuer et al. 2015) with an ex-vessel value of 93.8 million US dollars in 2014 (Fissel et al. 2015). Recruitment of this species is highly variable, therefore having the ability to identify all stages of development has potential utility for identifying spawning and nursery areas and estimating mortality rates between life stages. This knowledge could potentially support investigations of recruitment processes and stock structure that are crucial for proper management. The ability to distinguish the larvae of these three *Limanda* species will benefit studies of ichthyoplankton assemblage structure and species composition in the Arctic.

Methods

Field sampling

The study area is in the North Pacific Ocean, defined with a southern boundary in the Bering Sea at latitude 62°N and extending northward into the Chukchi (70°N, 180°W) and Beaufort seas (70°N, 150°W), which at present is the northern limit of our sampling (Fig. 1). This area is well within the boundary of the Arctic marine ichthyofaunal region as defined by Mecklenburg et al. (2011). In a few instances, material collected in the southern Bering Sea and Gulf of Alaska was used to fill gaps in developmental series. Most larvae were collected during 14 cruises from various studies conducted from 2004 to 2013 (Table 1). Gear used for collecting larvae and some early juveniles included a 60-cm bongo sampler fitted with 0.505-mm mesh nets (Posgay and Marak 1980), a 1-m^2 Tucker trawl that is a multi-net sampler that can be fished at specific depths and can also be used as an epibenthic sled (Tabery et al. 1977, referred to as "Tucker sled" in list of material examined) with 0.333 or 0.505-mm mesh nets, a modified beam trawl (MBT) with a 5-m^2 mouth opening fitted with a 3 × 2-mm oval mesh net and a 1-mm mesh cod end (Busby et al. 2014), and a modified Cantrawl fished as a surface or midwater trawl (Eisner et al. 2013). Bottom depth at most stations was 10–50 m. The Tucker sled was primarily intended to sample macrozooplankton near the bottom and in the water column as potential prey for baleen whales but was also found to be effective at catching larval and juvenile flatfish. Several types of bottom trawls were used to collect the juvenile and adult specimens used for radiographs.

Laboratory procedures

Ichthyoplankton samples collected during cruises listed in Table 1 were sorted, and larvae and juveniles were identified to the lowest taxonomic level possible (typically only to genus level for *Limanda* spp.) at the Plankton Sorting and Identification Center in Szczecin, Poland, using information in regional identification guides (Matarese et al. 1989; Ichthyoplankton Information System [IIS] 2015). Identifications were made to the species level by

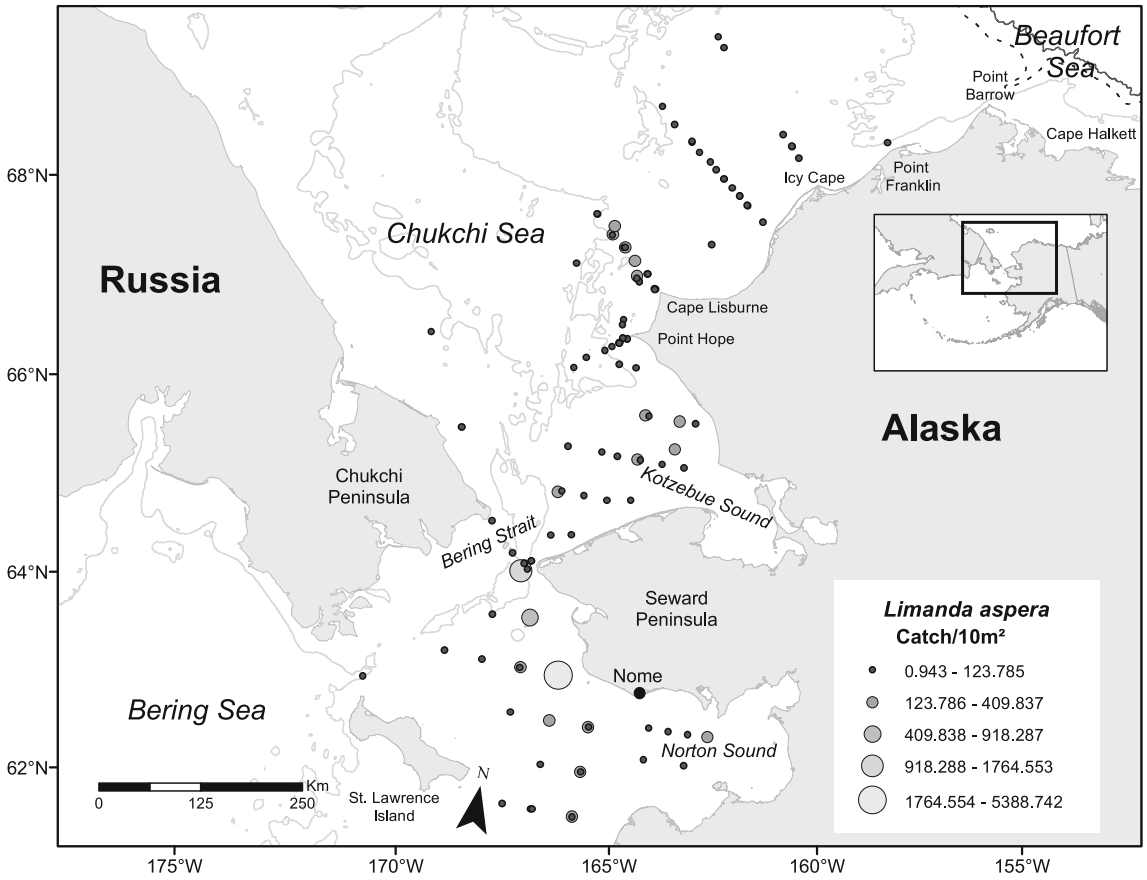

Fig. 1 Distribution and abundance of *Limanda aspera* larvae showing study area naming geographic features described in species accounts. Bathymetric contours are shown for 50 m (*gray lines*), 200 m (*black dotted lines*), and 1000 m (*black solid lines*). Inset shows location of study area expanded in the main map

Table 1 Cruises conducted within the study area

Cruise	Dates	Gear	No. of hauls	Location
1KR04	8/8/04–8/24/04	Bongo	18	Chukchi Sea
1SSO6	8/18/06–9/20/06	Bongo	30[a]	N Bering Sea
10M07	7/25/07–8/1/07	Modified beam trawl	6[b]	N Bering Sea
2DY07	9/5/07–9/25/07	Bongo	41	N Bering and Chukchi seas
10E08	8/6/08–8/22/08	Bongo	37	Beaufort Sea
1KR09	9/4/09–9/29/09	Bongo	33	Chukchi Sea
1AE10	8/27/10–9/14/10	Tucker sled	58	Chukchi Sea
1MB11	8/12/11–9/11/11	Tucker sled	64	Chukchi Sea
1BE12	8/7/12–8/22/12	Bongo	64	Chukchi Sea
2BE12	8/28/12–9/11/12	Bongo	43	N Bering and Chukchi seas
3BE12	9/12/12–9/24/12	Bongo	25[c]	N Bering Sea
1AQ12	8/17/12–8/27/12	Tucker sled	54	N Bering and Chukchi seas
1KR12	8/28/12–9/17/12	Bongo	20	Chukchi Sea
BE13-01	8/8/13–8/18/13	Bongo	42	N Bering and Chukchi seas

Some cruises sampled locations south of 62°N; only locations within the study area were considered. The area between 62°N and Bering Strait is considered to be the northern Bering Sea

[a] 99 stations were sampled overall; 30 were within study area

[b] 16 stations were sampled overall; 6 were within study area

[c] 35 stations were sampled overall; 25 were within study area

scientists at the AFSC in Seattle, WA, using a serial approach by which known juveniles identified using adult characters were linked to progressively smaller individuals by shared pigmentation and morphological characteristics (Busby 1998). One 37-mm total length (TL) postflexion-stage larva of *L. proboscidea* was identified using DNA barcoding techniques (Mecklenburg et al. 2011). The larva was collected in the eastern Chukchi Sea west of Kivalina, from a sample of five postflexion-stage specimens measuring 29–37 mm TL (CAS 230135). The adult it matched (collected during the same survey) is a 170-mm TL specimen collected south of Bering Strait near Sledge Island, west of Cape Rodney (CAS 230171; Mecklenburg et al. 2011). The postflexion-stage larvae represent a new record of occurrence of the species in the Chukchi Sea (Mecklenburg et al. 2011).

Developmental series were illustrated with a camera lucida attached to a dissecting microscope. Only melanistic pigment was described because formalin fails to preserve other color pigments. The best representative specimen of each taxon at each stage of development (preflexion, flexion, and postflexion) was illustrated. Transformation stages were illustrated if available. Because pigmentation among specimens was variable, some pigment described in the taxon accounts may not be visible on the illustrations. Morphometric measurements were taken on the right side of up to 50 larvae of each species, when possible, using a calibrated digital image-analysis system. Measurement definitions follow Matarese et al. (2013) except for body depth. Body depth 1 (BD1) is defined as the vertical distance from dorsal to ventral body margin through the base of the pectoral fin; body depth 2 (BD2), from the dorsal body margin to the center of the anus. All larval body lengths in this study are standard lengths unless otherwise noted; proportional lengths are expressed as percent standard length (SL) or head length (HL). All material used in this study is archived in the fish collections of the California Academy of Sciences (CAS) and the University of Washington (UW). Numbers given with these abbreviations are catalog numbers for the specimens in each respective collection. A complete list of material examined in this study is given in Online Resource 1.

Selected specimens were cleared and differentially stained using the method of Potthoff (1984) to count meristic structures and follow sequence of fin and vertebral column development. Most illustrated specimens and those used for morphometric measurements were not cleared and stained, and although their meristic counts fall within the overall ranges listed for each species (Table 2), individual counts from illustrations may differ from those found in the species-specific meristic tables generated from clearing and staining in this study. Terminology of osteological development follows Matarese et al. (2013). In descriptions of the development of meristic features, unossified precursors of fin and vertebral elements are classified as *visible*. *Differentiated* refers to the initial appearance of individual vertebral centra. In some cases, it was necessary to determine presence of a feature from unstained specimens. The term *developed* is used to indicate that the adult complement of fin elements, vertebral centra, or neural and haemal spines are completely formed but have not begun to ossify. Fins and vertebral elements are referred to as ossified upon initial uptake of alizarin red-s stain. The order of presentation of osteological descriptions is median fins, paired fins, and vertebrae, by sequence of ossification within each. For *L. sakhalinensis*, not all stages of development could be cleared and stained since the number of specimens was limited. Radiographs of adults obtained from the UW Fish Collection were used to obtain additional counts of meristic features.

Results

Limanda aspera

Larval distribution (Fig. 1)

Larvae of *Limanda aspera* are the most numerous and commonly occurring larvae of the three *Limanda* species found in Arctic waters. Larvae at lengths of 2.9–16.4 mm have been caught in August and September throughout the study area extending from St. Lawrence Island and Norton Sound in the northern Bering Sea to Point Franklin in the Chukchi Sea. Larvae have been collected at depths up to 56 m, with highest abundances near the western shore of Seward Peninsula.

Morphology (Tables 3, 4)

Notochord flexion in *L. aspera* begins at about 6–7 mm and is usually complete by about 9 mm. Postflexion-stage larvae are 8.9–18.7 mm. Transformation begins after 10.0 mm, and the juvenile stage begins by 28.0 mm. Relative head, snout, and snout-to-anus lengths increase with development. Relative body depth at the base of the pectoral fin and body depth at anus also increases and relative eye diameter decreases throughout development.

Pigmentation (Fig. 2)

In preflexion-stage larvae, head pigment is restricted to several melanophores along the angle of the lower jaw (Fig. 2a). The gut is pigmented dorsally along the hindgut and ventrally on the isthmus. A thin line of pigment extends along the ventral midline of the gut and some

Table 2 Meristic characters for the three Arctic *Limanda* species Sources: Mecklenburg et al. (2002) and this study

	n	Fins					Br	Vertebrae		
Taxon	Radiographs	Dorsal	Anal	Pectoral	Pelvic	Caudal		Precaudal	Caudal	Total
Limanda aspera	58	61–78	48–61	9–13	6	**2,7 + 9,0**	**7**	10–12	28–31	39–42[a]
Limanda proboscidea	19	61–77	45–58	9–13	6	**1–2,7 + 9,0**	**7–8**	10–12	26–30	36–40[b]
Limanda sakhalinensis	16	66–85	51–76	9–12	6–8	**4,6 + 9,0**	**7**	9–11	30–34	39–45

Br branchiostegal rays, *Underline* count is less or greater than previously reported, *Bold* first reported here

[a] *L. aspera* minimum total vertebrae 11 + 28 = 39, maximum 11 + 31 or 12 + 30 = 42 (this study)

[b] *L. proboscidea* minimum total vertebrae 10 + 27 or 11 + 26 = 37, maximum 11 + 29 = 40 (this study)

Table 3 Body proportions of *Limanda aspera* larvae

	Preflexion	Flexion	Postflexion
Sample size	17	15	16
Standard length (mm)	4.4 ± 0.7 (2.9–5.8)	6.8 ± 0.7 (5.7–8.0)	11.7 ± 2.3 (8.9–16.4)
Head length/SL	15.2 ± 1.7 (12.2–18.9)	19.4 ± 2.0 (15.4–22.2)	25.2 ± 1.5 (23.3–29.4)
Snout length/HL	19.5 ± 4.7 (8.8–26.7)	22.3 ± 4.7 (11.0–30.0)	22.8 ± 2.5 (16.5–26.4)
Eye diameter/HL	43.2 ± 3.6 (37.6–51.5)	32.5 ± 3.6 (28.1–41.3)	22.7 ± 2.0 (20.6–27.0)
Snout-to-anus length/SL	31.7 ± 1.7 (29.0–35.6)	32.9 ± 2.1 (28.3–36.8)	35.1 ± 3.0 (27.8–39.5)
Body depth 1/SL	13.1 ± 2.4 (9.1–18.6)	18.8 ± 2.1 (16.3–22.6)	28.0 ± 2.8 (24.7–34.1)
Body depth 2/SL	9.8 ± 1.3 (8.4–13.5)	15.4 ± 2.7 (12.2–21.1)	29.0 ± 3.4 (24.9–36.3)

Except for standard length (SL), values given for each body proportion are expressed as percentage of SL or head length (HL): mean ± standard deviation, and range (in parentheses)

melanophores may be present on either side of this line. Along the dorsal body, several melanophores are visible along the first few myomeres. On the postanal body, a row of melanophores occurs on either side of the ventral midline. Internal mediolateral pigment extends along the notochord beginning at about myomere 15 to the peduncle area and is sometimes irregularly spaced. Caudal pigment occurs in the finfold in the hypural area. In the early-flexion stage, larvae develop melanophores along the preopercular edge (Fig. 2b). Pigment on the gut increases ventrolaterally and on the isthmus; the ventral line becomes discontinuous. On the postanal body, slash-like pigment extends laterally along the hypaxial myomeres; this pigment is variable and can be restricted posteriorly along 5 myomeres or may be evenly spaced along the body on as few as 2 or as many as 15 myomeres. Internal mediolateral pigment may be discontinuous. Additional pigment is visible along the ventral and caudal finfold. Later flexion-stage larvae have increased pigmentation over the entire body (Fig. 2c). On the preanal body, pigment increases to the hindbrain, opercular area, isthmus, and jaw. Pigment on the gut increases laterally. On the postanal body, the internal pigment extends along the entire length of the notochord. Hypaxial pigment slashes extend along the myomeres and remain variable in number and placement. Additionally, pigment is scattered along the anal finfold and in the area where the caudal-fin rays are forming. Pigment change in postflexion-stage larvae occurs mainly along the postanal body (Fig. 2d). Internal notochord pigment becomes more embedded and difficult to see. A small line of pigment is present along the posterior end of the dorsal midline; the ventral midline pigment is darker directly opposite the dorsal midline pigment. As development progresses from postflexion to transformation stage, opposing dorsal and ventral midline pigment lines increase in width and number from posterior to anterior resulting in four dorsal and ventral opposing dark patches of melanophores; two additional dorsal midline pigment areas appear anteriorly (Fig. 2e). These patches on the dorsal and ventral body margins extend to, or are paired with, patches on the dorsal- and anal-fin rays and melanophores are scattered irregularly on the caudal-fin rays. The head and lateral surface of the gut become almost completely covered with melanophores. Epaxial and hypaxial pigmentation on the lateral body also greatly increases and the row of internal melanophores extends the entire length of the body. A row of hypaxial melanophores can be seen on the blind side of transformation-stage and early juvenile-stage individuals as can the internal row of melanophores above the notochord and the pigment patches on the dorsal and ventral body margins and fins.

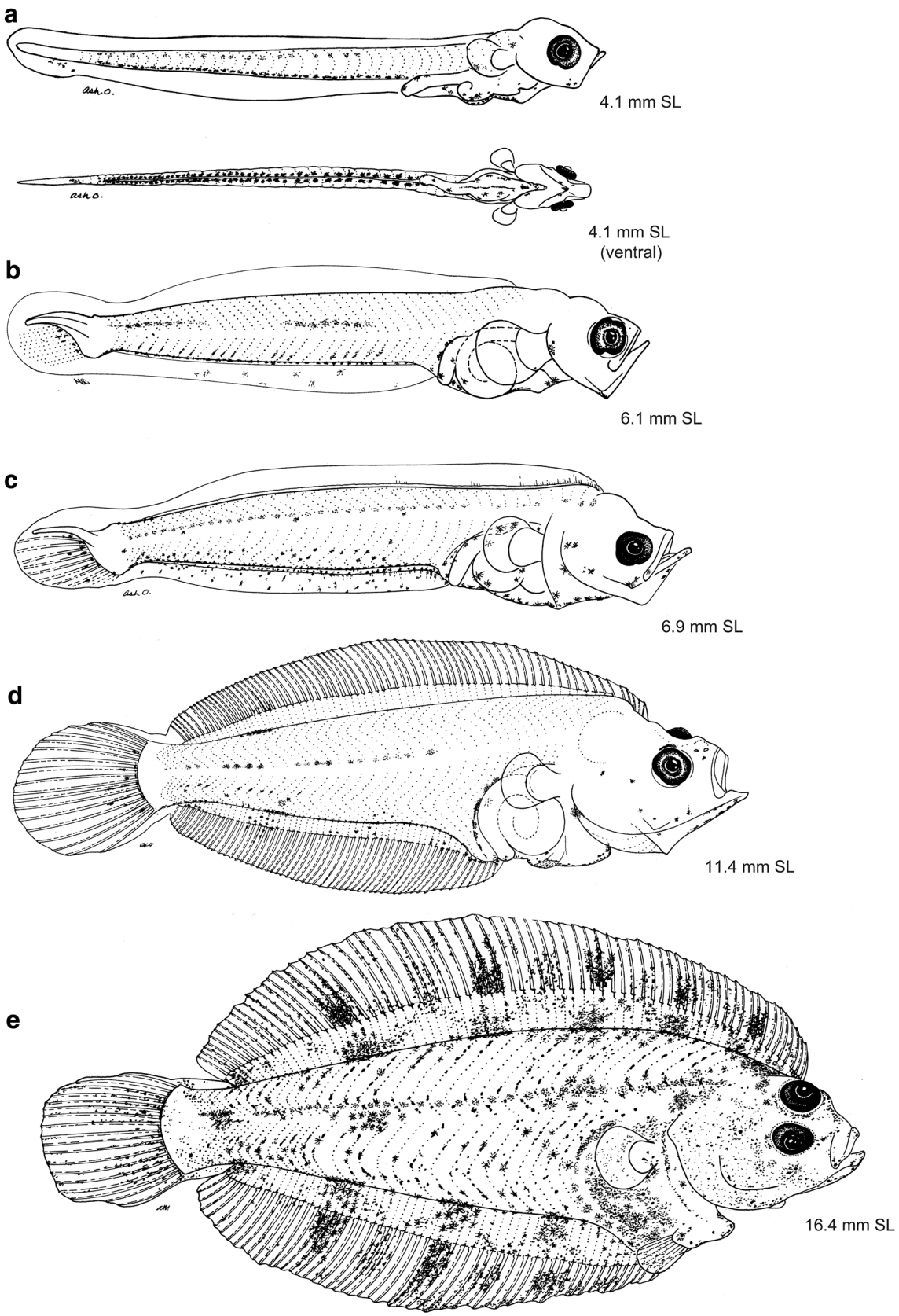

◀**Fig. 2** Development of *Limanda aspera* larvae. **a** Preflexion stage, UW 170966, 4.1 mm SL lateral and ventral views. **b** Flexion stage, UW 170968, 6.1 mm SL. **c** Flexion stage, UW 170967, 6.9 mm SL (Gulf of Alaska specimen). **d** Early transformation stage, UW 190969, 11.4 mm SL (southern Bering Sea specimen). **e** Transformation stage, UW 170963, 16.4 mm SL. Illustrations by A. Overdick

Meristic features (Table 4)

Principal caudal-fin rays are visible by 6.2 mm, developed by 10.1 mm, and ossified by 14.8 mm. Procurrent caudal-fin rays are visible by 8.9 mm, developed by 12.2 mm, and ossified by 14.8 mm. Dorsal- and anal-fin elements are visible by 7.3 mm, developed at 10.1–12.1 mm, and ossified at 14.8–18.7 mm. Pectoral-fin rays are not developed in transformation-stage larvae by 18.7 mm but are complete and ossified in juveniles at 28.0 mm. Pelvic-fin rays are visible at 12.1 mm, developed by 17.2 mm, and ossified by 18.7 mm. Vertebral centra begin to differentiate and neural and haemal spines are visible posteriorly at 6.2 mm. Ossification of vertebral centra, neural, and haemal spines can begin as early as 8.9 mm. All vertebral centra and neural and haemal spines are developed by 12.1 mm and ossified by 15.1 mm.

Limanda proboscidea

Larval distribution (Fig. 3)

Larvae of *Limanda proboscidea* have the widest distribution of Arctic species of *Limanda* from St. Lawrence Island to the Beaufort Sea. Longhead dab have been caught at lengths of 1.9–35.1 mm July–September in the northern Bering, Chukchi, and Beaufort seas, with highest abundances near Bering Strait, Kotzebue Sound, Point Hope, and Cape Lisburne at depths of 14–290 m.

Morphology (Tables 5, 6)

Notochord flexion in *L. proboscidea* begins at 7.0–8.0 mm and is complete by 12.0 mm. Postflexion-stage larvae are 10.2–35.1 mm. Transformation begins by 36.0 mm and the juvenile stage begins by 57.0 mm (larger than *L. aspera*, 28.0 mm). Relative head, snout, and snout-to-anus lengths increase with development. Both relative body depth at the base of the pectoral fin and body depth at anus increase throughout development and are greater at both flexion (mean of 24.0 and 23.2% SL, respectively) and postflexion stages (mean of 37.8 and 44.0% SL, respectively) than in other species of *Limanda*. Relative eye diameter decreases with development.

Pigmentation (Fig. 4)

Initially, preflexion-stage larvae have a melanophore on the lower jaw angle (Fig. 4a). The gut is pigmented along the dorsal and ventral surfaces. On the postanal body, a row of melanophores occurs on either side of the ventral midline. A few melanophores occur along the dorsal midline on the posteriormost third of the body. Below the dorsal midline pigment, several melanophores occur externally above the notochord. In the late preflexion stage, pigment is added to

Table 4 Counts of meristic characters of cleared and stained *Limanda aspera* larvae and juveniles

Standard length (mm)	Spines, rays				Branchiostegal rays	Neural spines			Haemal spines	Centra			Caudal-fin rays
	Dorsal fin	Anal fin	Pectoral fin	Pelvic fin		Abdominal	Caudal	Total		Abdominal	Caudal	Total	
5.0													
6.2													
6.2													
6.3													
6.6													
7.0													
7.3													
7.5													
8.9							27	27	27	3	27	30	
10.1						10	28	38	28				
11.4													
12.1						11	27	38	27				
12.2					7	11	25	36	25	11	25	36	
14.8	60	40			7	11	29	40	29	2	30	32	2,7+9,0
15.1					7	11	29	40	29	11	29	40	
17.2					7	11	29	40	29	11	30	41	2,7+9,0
18.7	66	47		6	7	10	29	39	29	10	30	40	2,7+9,0
28.0	**69**	**54**	**11**	**6**	**7**	**11**	**29**	**40**	**29**	**11**	**30**	**41**	-
51.4	**68**	**53**	**11**	**6**	**7**	**11**	**29**	**40**	**29**	**11**	**30**	**41**	**2,7+9,0**

- Character missing

Counts are of ossified elements only. Specimens between dashed lines are undergoing notochord flexion. *Bold* font indicates juveniles

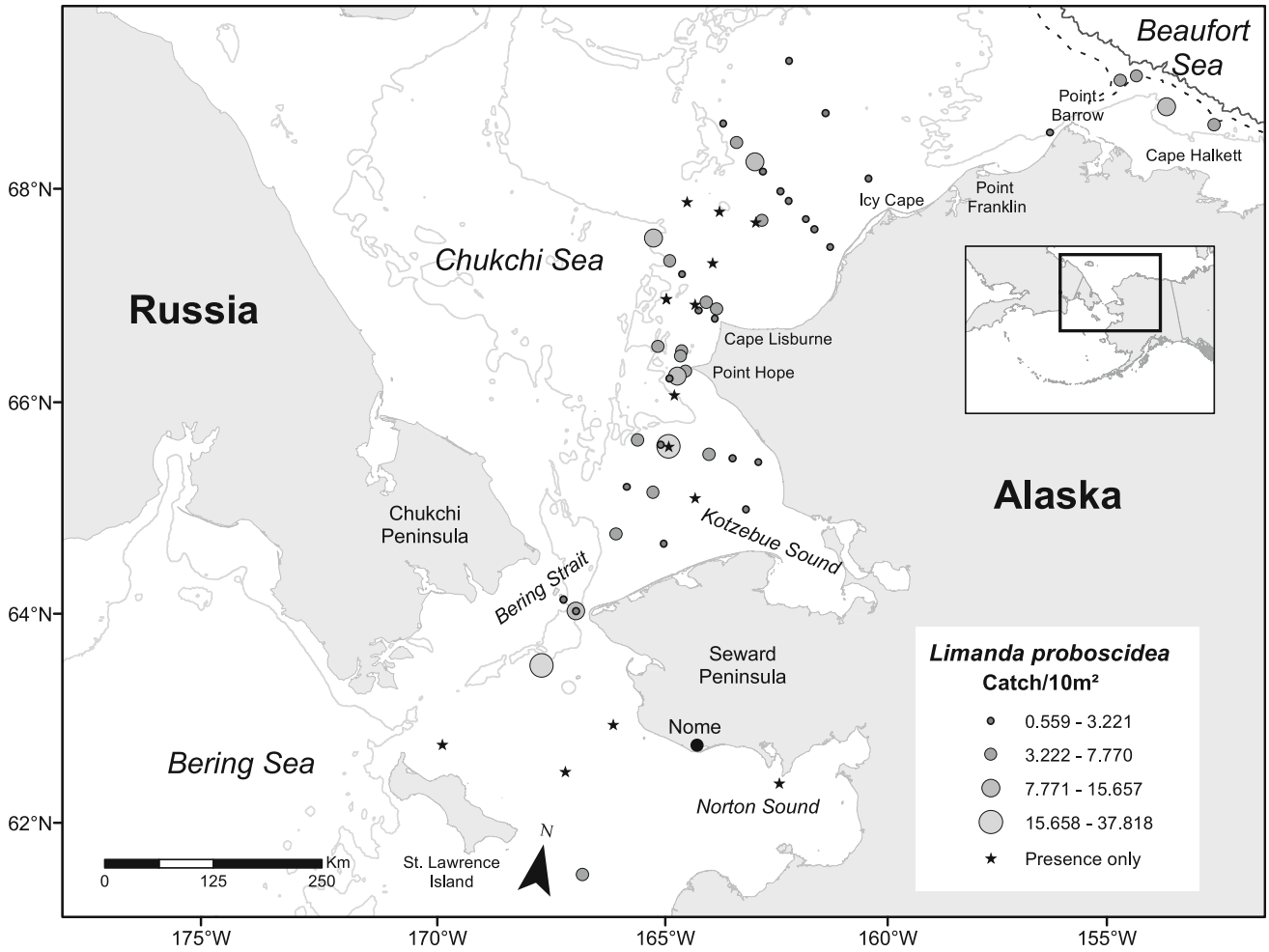

Fig. 3 Distribution and abundance of *Limanda proboscidea* larvae

Table 5 Body proportions of *Limanda proboscidea* larvae

	Preflexion	Flexion	Postflexion
Sample size	8	3	38
Standard length (mm)	3.4 ± 0.8 (1.9–4.4)	8.7 ± 0.8 (7.8–9.3)	18.8 ± 6.0 (10.2–35.1)
Head length/SL	12.9 ± 2.0 (9.7–15.6)	13.4 ± 0.7 (12.9–14.3)	27.9 ± 1.7 (21.8–32.0)
Snout length/HL	13.8 ± 4.0 (7.9–19.3)	21.5 ± 9.2 (11.0–28.1)	24.3 ± 2.6 (17.9–29.9)
Eye diameter/HL	61.4 ± 7.9 (49.0–73.8)	33.4 ± 2.6 (31.3–36.3)	23.1 ± 3.0 (15.0–28.2)
Snout-to-anus length/SL	35.6 ± 3.7 (32.4–43.5)	39.2 ± 2.1 (37.4–41.5)	40.1 ± 3.0 (33.6–45.3)
Body depth 1/SL	12.7 ± 2.5 (9.7–16.0)	24.0 ± 2.2 (21.5–25.3)	37.8 ± 3.2 (32.1–43.5)
Body depth 2/SL	8.6 ± 2.3 (5.0–12.7)[a]	23.2 ± 2.3 (20.7–25.2)	44.0 ± 5.2 (32.8–51.4)

Except for standard length (SL), values given for each body proportion are expressed as percentage of SL or head length (HL): mean ± standard deviation, and range (in parentheses)

[a] $n = 7$

the midbrain, jaw, cleithral area, and lateral surface of the hindgut (Fig. 4b). On the postanal body, an additional pairing of dorsal midline and above-notochord pigment develops anteriorly. The caudal area is unpigmented. On the preanal body in flexion-stage larvae, additional melanophores are present dorsally on the head, posterior edge of the opercle, cleithral area parallel with the ventral insertion of the pectoral-fin base, and jaw angle (Fig. 4c). A distinctive crescent of pigment is present posteriorly along the gut. On the postanal body, the dorsal midline, and mediolateral pigment above the notochord has expanded to include a ventral component now composed of epaxial and hypaxial pigment forming two weakly defined bars. A patch of pigment along the dorsal midline appears over the

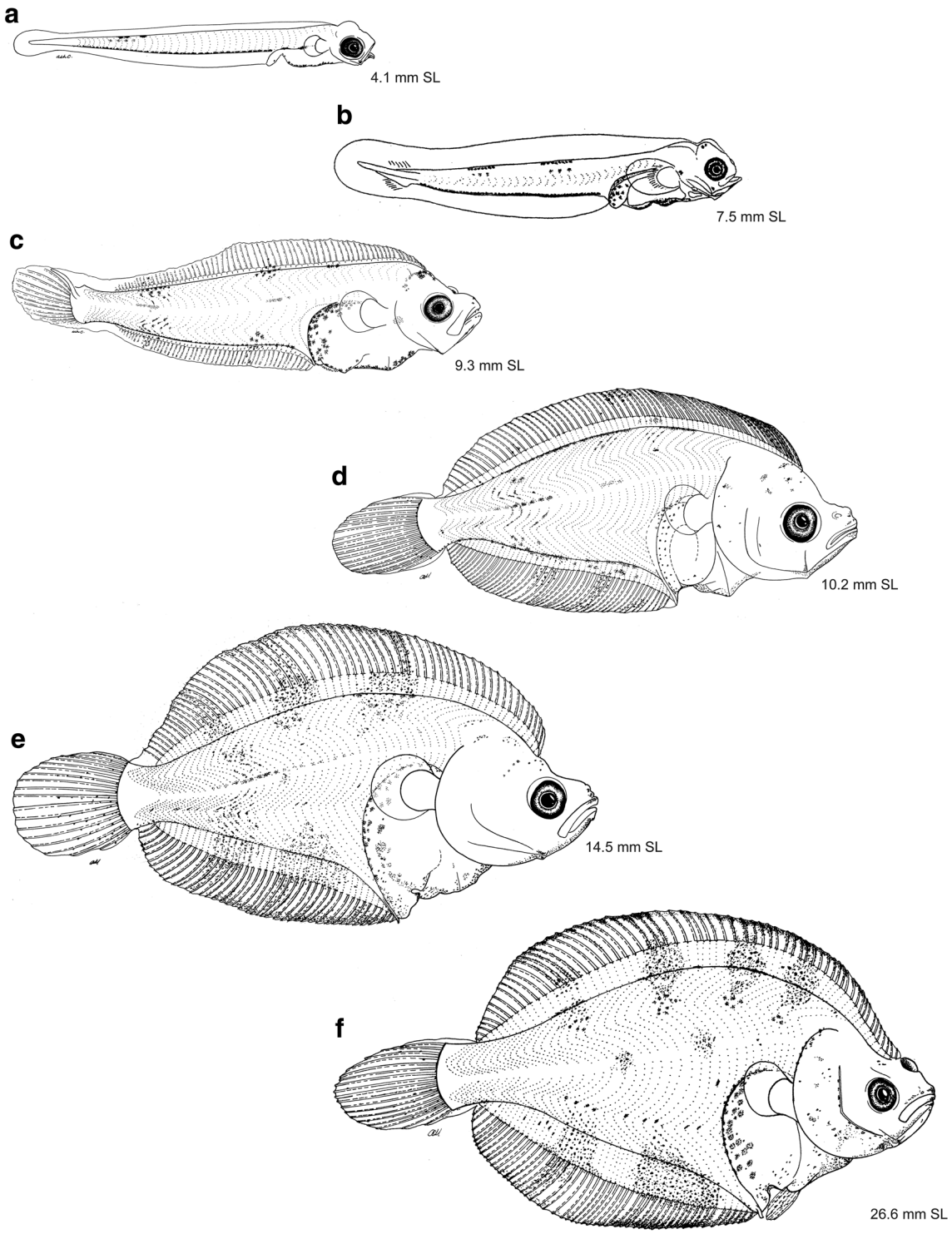

Fig. 4 Development of *Limanda proboscidea* larvae. **a** Preflexion stage, UW 171006, 4.1 mm SL. **b** Preflexion stage, 7.5 mm SL. **c** Flexion stage, UW 141002, 9.3 mm SL. **d** Postflexion stage, UW 171021, 10.2 mm SL. **e** Postflexion stage, UW 171022, 14.5 mm SL. **f** Early transformation stage, UW 171017, 26.6 mm SL. Illustrations (**a**, **c**–**f**) by A. Overdick and (**b**) from Grigor'ev (2004)

gut. Some pigment expands into the anal fin and posteriorly along the dorsal fin in line with the developing bars after 9.0 mm; additional pigment is on the first few rays of the anal fin. Postflexion-stage larvae have light head pigment with most melanophores occurring along the lower jaw and the cleithral area (Fig. 4d). The crescent of pigment posteriorly along the peritoneal cavity has become primarily internal. On the postanal body, the two bars and newly

formed anterior dorsal patch continue to develop and expand into the dorsal and anal fins. Pigment between the two bars along the dorsal midline is highly variable; a line of melanophores can connect them as early as 7.5 mm (flexion stage) and is complete by 10.2 mm (Fig. 4d). The edge of the dorsal fin is pigmented anteriorly to the medial patch, then later extends to the posteriormost patch. Pigment along the distal edge of the dorsal fin is also highly variable and can connect anterior and posterior patches in larvae 10.2–14.5 mm. A thin but dark line of melanophores is present on the distal edge of the anal fin anteriorly in larvae about 14.5 mm and larger. In larvae 10.2–14.5 mm, slash-like melanophores are present on the hypaxial area of the caudal peduncle (Figs. 4d, e). Transforming larvae are generally more pigmented over the entire body (Fig. 4f). More pigment occurs on the head along the upper jaw and opercular and cleithral areas. An additional dorsal patch develops anteriorly over the pectoral fin.

Meristic features (Table 6)

Principal caudal-fin rays are visible at 7.0 mm, developed by 10.2 mm, begin to ossify by 15.8 mm, and are completely ossified at 25.0 mm. Procurrent caudal-fin rays are visible by 9.3 mm and are developed and ossified by 25.0 mm. Although the illustration of a 7.5 mm preflexion-stage larva from Grigor'ev (2004, Fig. 5b) shows what appear to be superior procurrent caudal-fin rays, none of our specimens possess these elements. Dorsal- and anal-fin elements are visible by 9.3 mm, developed from 10.2 to 12.1 mm, and ossify at 15.8–25.0 mm. Pectoral-fin rays begin to develop at 36.0 mm and are complete and ossified at 57.0 mm. Pelvic-fin base and early rays are visible at 10.2 mm (Fig. 4d), developed by 17.5 mm, and ossified by 36.0 mm. Neural and haemal spines begin to form posteriorly and are complete by 9.3 mm and vertebral centra are differentiated by 10.6 mm. All vertebral centra and neural and haemal spines are developed by 12.0 mm and may be ossified as early as 15.8 mm.

Limanda sakhalinensis

Larval distribution (Fig. 5)

Larvae of *Limanda sakhalinensis* are the least abundant of the three species of *Limanda* in our study area. Most have been collected at lengths of 6.3–15.1 mm during August and September in or near Kotzebue Sound, with other occurrences in the northern Bering Sea, Bering Strait, and off Point Hope and Cape Lisburne at depths of 24–48 m.

Morphology (Table 7)

Notochord flexion in *L. sakhalinensis* begins at about 6 mm and is complete by 10.5 mm. Postflexion-stage larvae are 10.0–15.1 mm. Eye migration is evident in our largest larva, thus transformation had begun by 15.1 mm. It is unknown when the juvenile stage begins. Although there was only one preflexion-stage larva, it appears that relative head length and snout-to-anus length increase with development. Relative body depth at the base of the pectoral fin and body depth at anus also increase with development and are smaller at both flexion (mean of 16.8 and 13.5% SL,

Table 6 Counts of meristic characters of cleared and stained *Limanda proboscidea* larvae and juveniles

Standard length (mm)	Spines, rays				Branchiostegal rays	Neural spines			Haemal spines	Centra			Caudal-fin rays
	Dorsal fin	Anal fin	Pectoral fin	Pelvic fin		Abdominal	Caudal	Total		Abdominal	Caudal	Total	
5.6													
6.6													
7.0													
8.0													
9.3													
10.6													
11.3													
12.0													
15.8	15	15			7	11	28	39	23	11	27	38	1,7+8,0
17.5		5			7	4	4	8	10				
25.0	65	48	-	5	7	11	27	38	26	11	27	38	2,7+9,0
29.2					8	11	27	38	27	11	28	39	-
36.0	68	50		6	7	11	28	39	27	11	29	40	1,8+9,0
57.0	**68**	**52**	**13**	**6**	**7**	**11**	**27**	**38**	**27**	**11**	**28**	**39**	**1,8+9,0**
90.0	**64**	**47**	**11**	**6**	**7**	**11**	**26**	**37**	**26**	**11**	**27**	**38**	**1,8+9,0**

Counts are of ossified elements only. Specimens between dashed lines are undergoing notochord flexion. *Bold* font indicates juveniles

- Character missing or damaged

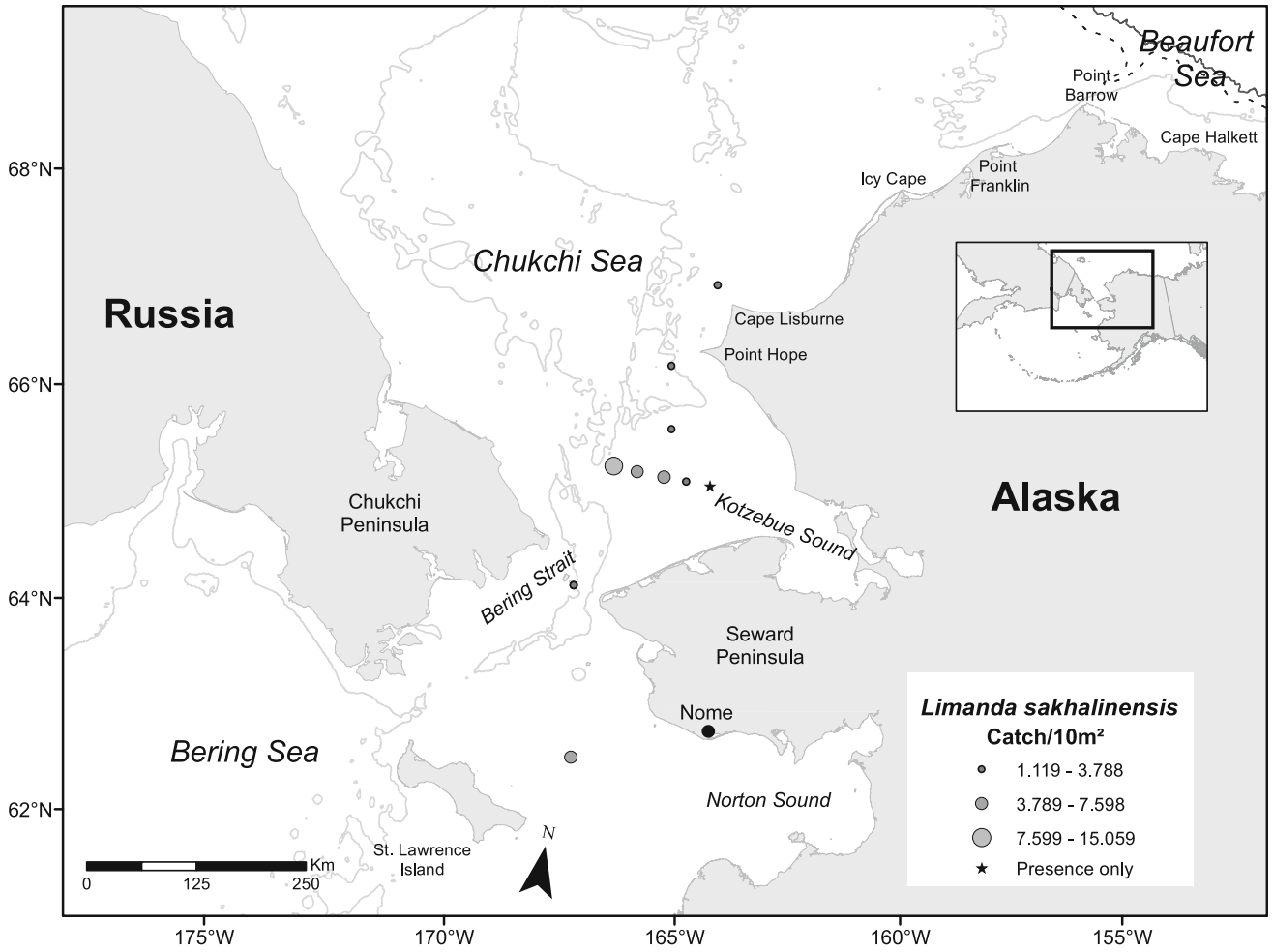

Fig. 5 Distribution and abundance of *Limanda sakhalinensis* larvae

Table 7 Body proportions of *Limanda sakhalinensis* larvae

	Preflexion	Flexion	Postflexion
Sample size	1	14	4
Standard length (mm)	6.6	8.2 ± 1.3 (6.3 – 10.5)	12.2 ± 2.2 (10.0 – 15.1)
Head length/SL	15.1	19.3 ± 2.3 (15.6 – 22.9)	22.0 ± 1.9 (19.9 – 24.3)
Snout length/HL	–[a]	22.4 ± 5.3 (11.4 – 27.0)[b]	21.4 ± 4.4 (17.2 – 25.2)
Eye diameter/HL	–[a]	31.2 ± 3.5 (25.2 – 35.7)[b]	25.9 ± 1.7 (23.4 – 27.5)
Snout-to-anus length/SL	26.4	33.1 ± 2.1 (29.0 – 35.7)[b]	34.9 ± 2.8 (31.6 – 38.6)
Body depth 1/SL	13.5	16.8 ± 1.6 (14.4 – 19.2)	20.6 ± 2.3 (17.9 – 22.9)
Body depth 2/SL	9.9	13.5 ± 2.9 (9.4 – 19.0)	20.6 ± 2.7 (16.6 – 22.8)

Except for standard length (SL), values given for each body proportion are expressed as percentage of SL or head length (HL): mean ± standard deviation, and range (in parentheses)

[a] $n = 0$

[b] $n = 13$

respectively) and postflexion stages (mean of 20.6% SL for both measurements) than other species of *Limanda*. Relative snout length and eye diameter were not available from the preflexion larva but decrease from flexion to postflexion stages.

Pigmentation (Fig. 6)

Head pigment in early-flexion-stage larvae consists of several melanophores along the lower jaw and a single melanophore on the midbrain (Fig. 6a). The gut is

pigmented ventrally on the isthmus and midgut and dorsally along the hindgut. On the postanal body, pigment extends laterally along the hypaxial myomeres. Internal mediolateral pigment extends along the notochord beginning at about myomere 12 to the caudal peduncle. Fine pigment outlines the dorsal margin of the notochord in the caudal area, wraps around to its ventral margin, and continues along the posterior edge of the developing hypural plates. Head pigment increases in flexion-stage larvae with pigment on the jaw margin and in the opercular area; pigment on the midbrain is prominent (Fig. 6b). On the preanal body, additional pigment occurs at the base of the cleithrum, laterally on the gut and hindgut, and on the ventral portion of the pectoral-fin base. On the postanal body, the internal pigment along the notochord extends anteriorly to about myomere 4. Hypaxial pigment is heavier and there is a row of melanophores along the length of the developing anal-fin pterygiophores. Pigment is scattered in the area where the caudal-fin rays are forming. Pigment continues to increase in postflexion-stage larvae. Additional melanophores appear on the head and snout, anterior margin of the eye, and on the jaw angle; however, opercular pigment that had developed during the flexion stage is not visible in postflexion-stage larvae (Fig. 6c). The prominent pigment on the midbrain becomes embedded; most is around the base or posterior margin and increases with development. On the preanal body, additional pigment is visible on the isthmus and in the cleithral area. Internal mediolateral pigment extends the entire length of the notochord. Additional pigment on the postanal body appears along the dorsal-fin pterygiophores and onto the developing dorsal-fin rays starting at about mid-body; pigment extends onto the developing fin rays along most of the length of the anal fin. Additional pigment along the lower jaw is seen in late postflexion-stage larvae, along with light scattered melanophores on the cheek and

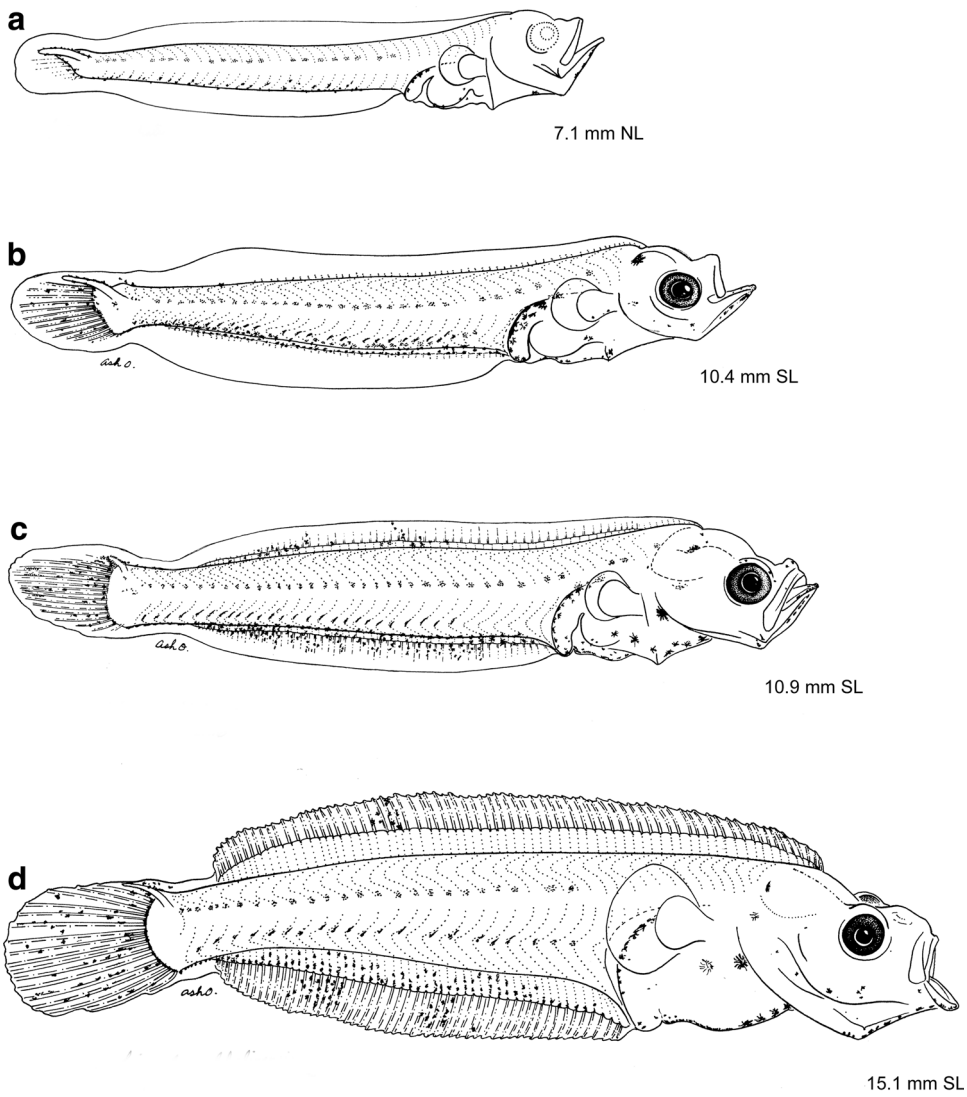

Fig. 6 Development of *Limanda sakhalinensis* larvae. **a** Early flexion stage, UW 171031, 7.1 mm SL. **b** Flexion stage, UW 171026, 10.4 mm SL. **c** Postflexion stage, UW 171027, 10.9 mm SL. **d** Early transformation stage, UW 171035, 15.1 mm SL. Illustrations by A. Overdick

operculum (Fig. 6d). A row of melanophores extends along the ventral midline of the gut. The internal mediolateral pigment above the notochord is visible only on the postanal body. Pigment on the dorsal fin is restricted to one patch on the rays just posterior to midbody; all anal-fin pterygiophores are pigmented, but pigment on the anal-fin rays is restricted to two patches that are anterior and posterior to the dorsal-fin patch. Pigment outlines the posterior margin of the caudal body and additional melanophores are present on the caudal-fin rays.

Meristic features (Table 8)

Principal caudal-fin rays are developed but unossified by 8.0 mm, begin to ossify by 9.4 mm, and are completely ossified at 11.1 mm. Procurrent caudal-fin rays are developed and ossified by 11.1 mm. Dorsal- and anal-fin elements are visible anteriorly at 8.0 mm and nearly all are ossified at 11.1 mm. Pectoral-fin rays are not visible by 15.1 mm but are developed and likely ossified at 48.0 mm (Fig. 6d). This observation is based on a poorly preserved juvenile-stage specimen that did not take up alizarin red-s stain. We could not determine from our material when pelvic-fin rays are first visible, but they are developed by 48.0 mm and ossified by 87.0 mm. Vertebral centra begin to differentiate and all neural and haemal spines are developed at 8.0 mm. All vertebral centra and neural and haemal spines are developed and ossified by 11.1 mm.

Discussion

Species comparisons

Primary characters that distinguish larvae of the three species of *Limanda* are pigmentation, body depth, and length of larvae and early juveniles at developmental stage landmarks (Online Resource 2). Early-stage larvae of *Limanda aspera* and *L. sakhalinensis* both have slash-like hypaxial melanophores and a row of internal melanophores dorsally along the notochord. In contrast, *L. sakhalinensis* larvae have pigment around the notochord tip and posterior edge of the developing hypural plates that is absent in *L. aspera*. Preflexion-stage larvae of *L. proboscidea* lack the slash-like hypaxial melanophores present in *L. aspera* and *L. sakhalinensis* but have pigment along the dorsal margin of the posterior body that is absent in the other two species. Flexion- and postflexion-stage *L. proboscidea* larvae have pigment patches along the dorsal and ventral margins of the body and a vertical pigment band on the posterior lateral body that are absent in *L. aspera* and *L. sakhalinensis*. Pigmentation of early transformation-stage larvae is very similar to that seen in postflexion-stage larvae for all three species (Figs. 2d, 4e, 6d). Late transformation/early juvenile stages are only known for *L. aspera* and pigmentation is composed of large clusters of melanophores on the dorsal and anal fins, body, and body margins with a row of single melanophores along the lateral line (Fig. 2e). Additional melanophores are scattered over the lateral body and slash-like hypaxial pigmentation remains as seen in previous stages.

Notochord flexion in *L. aspera* begins at about 6–7 mm and is complete around 10 mm, while in *L. proboscidea* it begins at about 8 mm and is complete by 12 mm. Flexion in *L. sakhalinensis* begins at about 6 mm and is complete by 10.5 mm. Transformation, characterized initially by the beginning of eye migration, starts at about 10–13 mm for *L. aspera*, 15 mm for *L. sakhalinensis*, and 26 mm for *L. proboscidea*.

Relative body depth at the pectoral-fin base and body depth at the anus increase throughout development and are greater in both flexion and postflexion stages. Preflexion-stage larvae of all three species are slender-bodied, with mean BD1 about 13% and BD2 roughly 9%. Flexion and postflexion-stage larvae of *L. proboscidea* have greater mean body depth (e.g., postflexion-stage 37.8% BD1, 44.0% BD2/SL *L. proboscidea* vs. 28.0% BD1, 29.0% BD2/SL *L. aspera* and 20.6% BD1, 20.6% BD2/SL *L. sakhalinensis*) (Tables 3, 5 and 7).

Table 8 Counts of meristic characters of cleared and stained *Limanda sakhalinensis* larvae and juveniles

Standard length (mm)	Spines, rays: Dorsal fin	Anal fin	Pectoral fin	Pelvic fin	Branchiostegal rays	Neural spines: Abdominal	Caudal	Total	Haemal spines	Centra: Abdominal	Caudal	Total	Caudal-fin rays
8.0													
9.4									15		1	1	6+7
11.1	73	54				10	31	41	31	10	32	42	4,6+9
48.0 [a]	***75***	***58***	***12***	***6***	***6?*** [b]	***11***	***28***	***39***	***28***	***11***	***29***	***40***	***3,6+9,0***
87.0	**73**	**59**	**12**	**6**	**7**	**10**	**31**	**41**	**31**	**10**	**32**	**42**	**3,6+9,0**

Counts are of ossified elements only except the 48.0 mm SL specimen. Specimens above dashed line are undergoing notochord flexion. *Bold* font indicates juveniles. *Italic* font indicates no uptake of alizarin stain, probably due to inadequate preservation

[a] Counts are of unstained elements. Specimen is clearly a juvenile

[b] Count is uncertain

Larvae of some other North Pacific pleuronectid genera bear a striking resemblance to those of *Limanda* and can be difficult to distinguish in samples where they co-occur. Preflexion-stage larvae of both *Limanda aspera* and *Pleuronectes quadrituberculatus* (Alaska plaice; Fig. 7a) have a double row (one row on each side of the ventral midline) of postanal ventral melanophores (PVM) and an imbedded (internal) row of melanophores posteriorly above the notochord. However, preflexion-stage *P. quadrituberculatus* differ from *L. aspera* by having two or more melanophores on the dorsal midline posteriorly, more preanal myomeres (12–14 vs. 10–12), and hatching at a larger size (4.6 mm vs. 2.9 mm). Flexion- and postflexion-stage *L. aspera* larvae have slash-like hypaxial melanophores that are absent in *P. quadrituberculatus*. During transformation, eyes begin migrating by 10–11 mm in both species and are usually complete by 15–16 mm, which is small in comparison to many other pleuronectids (see IIS 2015).

In contrast to the other two species of *Limanda* described here, larvae of *Limanda proboscidea* are more similar in appearance to larvae of the three species of *Lepidopsetta*; *L. bilineata*, *L. mochigarei*, *L. polyxystra* (southern rock sole, ricecake sole and northern rock sole; Fig. 7b, only *L. polyxystra* shown) (Orr and Matarese 2000), and *Psettichthys melanostictus* (sand sole, Fig. 7c) (Matarese et al. 1989). All have two or more patches of melanophores on the dorsal body margin in flexion and later stages and a vertical band of pigmentation on the posterior body that are absent in the other two species of *Limanda*. Various patterns of melanophores are present in the finfolds of preflexion-stage larvae of *Lepidopsetta* and *Psettichthys* that are absent in *L. proboscidea*. In postflexion-stage larvae, patches of pigment are present on the rays of the dorsal and anal fins in *L. proboscidea* and a streak of pigmentation on the distal margin of the anterior dorsal fin very similar to that seen in *P. melanostictus* is present (Fig. 7c). Initially we had considered postflexion-stage *L. proboscidea* larvae to be those of *Pleuronectes glacialis* (Arctic flounder), but the anal-fin ray counts are too high (45–58 *L. proboscidea* vs. 33–46 *P. glacialis*) and a DNA barcode match further verified the identifications (Mecklenburg et al. 2011).

We initially identified two flexion-stage larvae collected off Norton Sound as *Acanthopsetta nadeshneyi* (spiny flounder) based on the descriptions and illustrations of Pertseva-Ostroumova (1961). However, additional investigation and discussions with other researchers revealed that *A. nadeshneyi* is not an Arctic species (Mecklenburg et al. 2011). An adult specimen of *A. nadeshneyi* reported from Cape Navarin by Lindberg and Fedorov (1993) is a misidentified *L. sakhalinensis* initially from Taranetz (1937) (pers. comm. B. Sheiko, Zoological Institute, St. Petersburg, Russia, Jan. 2012). This information and similarities in pigmentation to *L. aspera* led us to identify these larvae as *L. sakhalinensis*. Larvae of *L. sakhalinensis* are also similar in appearance to *Parophrys vetulus* (English sole, Fig. 7d), having internal melanophores above the notochord or vertebral column, slash-like hypaxial pigmentation, and melanophores around the notochord tip. Early larvae of *P. vetulus*, however, have a more rounded snout and melanophores on the dorsal midline and the anal finfold that are absent in *L. sakhalinensis*. In addition it is important to note that the known distribution of *P. vetulus* precludes them from areas where *L. sakhalinensis* occur.

Phylogenetic relationships

In their analysis of the family Pleuronectidae using adult characters, Cooper and Chapleau (1998) were unable to resolve monophyly and intra-relationships of the genus *Limanda*. Early-life-history characters were not considered in their analysis. Marine fish larvae possess characters that are uniquely evolved adaptations for planktonic life that are independent of adult characters and useful in studies of phylogenetic relationships (Moser 1981). Placed in tribe Pleuronectini (subfamily Pleuronectinae), with *Parophrys*, *Platichthys*, *Pleuronectes*, and *Pseudopleuronectes*, larvae of *L. aspera* and *L. sakhalinensis* share several characters with these genera including slash-like hypaxial pigmentation, pigment on the finfolds or fin rays, small size at transformation, and have relatively slender bodies during the postflexion stage compared to other pleuronectid flatfish. However, larvae of *L. proboscidea* are more similar in appearance to genera in tribes Psettichthyini (*Psettichthys*) and Microstomini (*Lepidopsetta*) as previously noted. The deep body with crescent-shaped pigment around the gut, pigment streaks on the distal margins of the dorsal and anal fins, and vertical band on the caudal peduncle area (posterior body) of flexion- and postflexion-stage *L. proboscidea* is very similar to *Psettichthys melanostictus*. The deep, rather circular-shaped body and large size at transformation of *L. proboscidea* is similar to that of *Microstomus* (see Matarese et al. 1989) and is consistently deeper than the other two species of *Limanda* throughout development. Using both molecular and larval characters including pigmentation, the analysis of Roje (2010) recovered a clade comprised of *L. proboscidea* with *Pseudopleuronectes, Pleuronectes*, *Platichthys*, *Lepidopsetta*, *Parophrys, Isopsetta*, and *Psettichthys* while *L. aspera* and *L. sakhalinensis* were recovered in a separate clade with the genera *Hippoglossoides*, *Cleisthenes* (subfamily Hippoglossoidinae), and *Dexistes* (subfamily Pleuronectinae), further supporting paraphyly of the genus *Limanda*.

Classification of the righteye flounders, family Pleuronectidae, has been recently reviewed and changes were

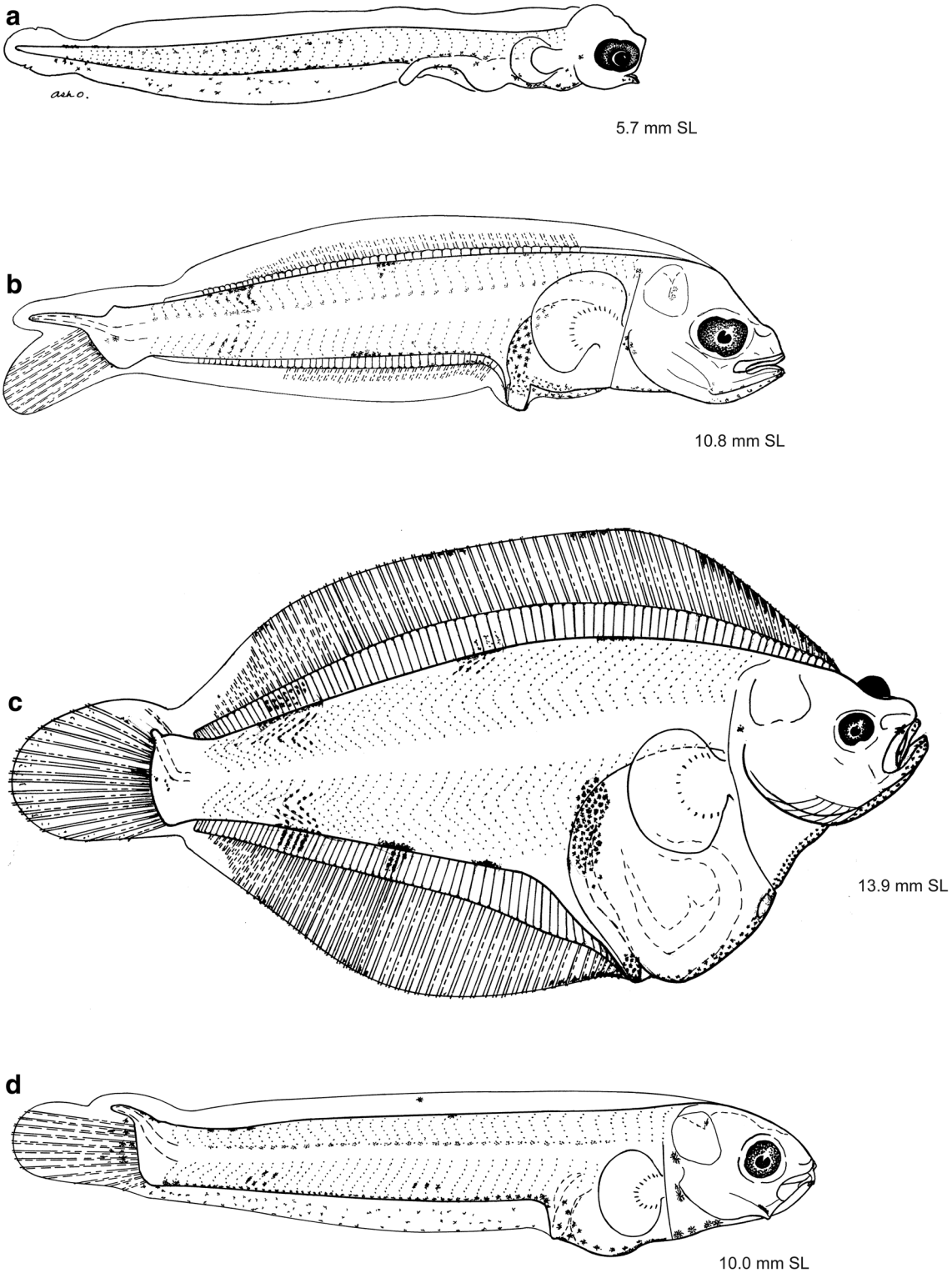

Fig. 7 Larvae of flatfish species that resemble *Limanda aspera*, *L. proboscidea*, or *L. sakhalinensis*. **a** *Pleuronectes quadrituberculatus* preflexion stage, UW 167588, 5.7 mm SL. **b** *Lepidopsetta polyxystra* flexion larva, 10.8 mm SL. **c** *Psettichthys melanostictus* postflexion stage, 13.9 mm SL. **d** *Parophrys vetulus* flexion stage, 10.0 mm SL. Illustrations (**a**) from IIS (2015), (**b**) from Orr and Matarese (2000), and (**c**–**d**) from Matarese et al. (1989)

proposed involving Pacific Arctic flounders (Mecklenburg and Steinke 2015) including generic names of species in *Limanda.* Historically, longhead dab has been classified as *Limanda proboscidea* (e.g., Cooper and Chapleau 1998; Mecklenburg et al. 2002; Nelson 2006; Page et al. 2013; Mecklenburg et al. 2013). However, comparisons of DNA sequence data support a different classification that resurrects Gill's (1861) genus *Myzopsetta* for *L. proboscidea* and two Atlantic species currently placed in *Limanda* (Mecklenburg and Steinke 2015). Andriashev (1954) and Lindberg and Fedorov (1993) distinguished two species groups in the genus *Limanda* and Andriashev (1954) recognized *Myzopsetta* as a subgenus including *L. ferruginea*, *L. punctatissima*, and *L. proboscidea*. Sheiko and Fedorov (2000) treated *Myzopsetta* as a full genus in their checklist of Kamchatka fishes. McCusker et al. (2013) found that DNA sequences from four of the *Limanda* species also fell into two major groups. With this taken into consideration, a revision of the genus *Limanda* is needed and we add to the support for restoring the genus *Myzopsetta.*

Concluding remarks

With the exception of late transformation/early juvenile-stage *L. sakhalinensis*, our study has provided descriptions of nearly all stages of larval development for the three species of *Limanda* occurring in the Pacific Arctic Basin that can be used to accurately identify specimens collected in ecological and environmental impact studies. Larvae of *L. aspera* were second in overall abundance only to the gadid *Boreogadus saida* (Arctic cod) (Norcross et al. 2010) in a 2004 ichthyoplankton survey and the most abundant species in all other surveys 2007–2011 (Logerwell et al. 2015). Thus it is clear that *L. aspera* is a dominant member of the Chukchi Sea ichthyoplankton community and important in energy transfer from lower to upper trophic levels. As the target of a large commercial fishery, it is important to note that the northern Bering and Chukchi Seas are the northern limits of the known range of *L. aspera* and with current warming trends in the Arctic Ocean Basin, northward range expansion is a distinct possibility (Nye 2009). With this in mind, there is potential for commercial fishing fleets to follow this fishery northward if allowed by the North Pacific Fishery Management Council (NPFMC). Data collected on recent ichthyoplankton surveys in the Chukchi Sea have identified potential *L. aspera* spawning areas based on collections of pelagic eggs. However, the distribution of larvae appears to vary between years depending on prevailing circulation patterns (Busby et al. 2015). In addition, larvae of the three *Limanda* species have been identified as members of distinct ichthyoplankton assemblages. As analyses of currently archived data and additional surveys continue, our understanding of the complexities of the Pacific Arctic ecosystem and the life history, distribution, and identification of Arctic ichthyoplankton and climate-mediated impacts on fish populations will undoubtedly increase.

Acknowledgements AA Overdick (formerly AFSC) illustrated all *Limanda* specimens with the exception of Fig. 4b (from Grigor'ev 2004). She also illustrated the preflexion-stage *Pleuronectes quadrituberculatus* larva shown in Fig. 7a and assisted with preparing radiographs and counting meristic features. LG De Forest (formerly AFSC) compiled adult meristic data and measured morphometric features. JR Randall (AFSC) assisted with listing material examined, preparing radiographs, compiling counts of meristic features and reviewed an earlier draft of the manuscript. The authors thank CW Mecklenburg (CAS) and TK Wilderbuer (AFSC) for general assistance, and JW Orr (AFSC) for reviewing an early draft of the manuscript. Specimens used in this study include those collected during the Chukchi Sea Acoustics, Oceanography, and Zooplankton (CHAOZ) Study, OCS Study BOEM 2015-034, funded by the Bureau of Ocean Energy Management under Interagency Agreement #M09PG00016, Arctic Ecosystem Integrated Survey (Arctic Eis) OCS Number: 2011-AK-11-08a/b Agreement #M12PG00018, and the 2004–2012 surveys of the Russian-American Long-Term Census of the Arctic (RUSALCA) Program funded by the NOAA Arctic Research Program under cooperative agreement NA17RJ1224 with the University of Alaska. This is contribution EcoFOCI-N877 to NOAA's North Pacific Climate Regimes and Ecosystem Productivity research program.

References

Andriashev AP (1954) Fishes of the northern seas of the U.S.S.R. *Opredeliteli po Faune SSSR* 53. Akademii Nauk SSSR, Moscow, p 567 [In Russian; and English translation, 1964, Israel Program for Scientific Translations, p 617]

Busby MS (1998) Guide to the identification of larval and early juvenile poachers (Scorpaeniformes: Agonidae) in the Northeast Pacific Ocean and Bering Sea. NOAA Technical Report NMFS 137, p 88

Busby MS, Duffy-Anderson JT, Mier KL, De Forest LG (2014) Summer ichthyoplankton assemblages on the eastern Bering Sea shelf. Fish Oceanogr 23:270–287

Busby MS, Duffy-Anderson JT, Mier KL, Tabisola HM (2015) Ichthyoplankton assemblages and distribution patterns in the Chukchi Sea (2012–2013). Arctic Eis Final Report. BOEM US Department of the Interior, Bureau of Ocean Energy Management, Alaska OCS Region. OCS Study BOEM 2011-AK-11-08 a/b. p 38

Cooper AJ, Chapleau F (1998) Monophyly and intrarelationships of the family Pleuronectidae (Pleuronectiformes), with a revised classification. Fishery Bull US 96:686–726

Eisner L, Hillgruber N, Martinson E, Maselko J (2013) Pelagic fish and zooplankton species assemblages in relation to water mass characteristics in the northern Bering and southeast Chukchi seas. Polar Biol 36(1):87–113

Fissel B, Dalton M, Felthoven R, Garber-Yonts B, Haynie A, Himes-Cornell A, Kaperski S, Lee J, Lew D, Seung, C (2015) Stock assessment and fishery evaluation report for the groundfish fisheries of the Gulf of Alaska and Bering Sea/Aleutian Islands Area: economic status of the groundfish fisheries off Alaska. North Pacific Fishery Management Council, Anchorage, AK 99510, p 406

Gill TN (1861) Catalogue of the fishes of the eastern coast of North America, from Greenland to Georgia. Proc Acad Nat Sci Phila 13:1–63

Grigor'ev SS (2004) Description of the longhead dab *Limanda proboscidea* (Pleuronectidae) larvae from the Sea of Okhotsk. J Ichthyol 44:152–157

Ichthyoplankton Information System (IIS) (2015) Nat Oceanic Atmos Admin. http://access.afsc.noaa.gov/ichthyo/index/php. Accessed 14 June 2016

Lindberg GU, Fedorov VV (1993) Fishes of Japan Sea and nearby parts of Okhotsk and Yellow seas. Part 6. Teleostomi. Osteichthyes. Actinopterigii. XXXI. Pleuronectiformes. Sankt-Petersburg University Press, Sankt-Petersburg, p 272

Logerwell E, Busby M, Carothers C, Cotton S, Duffy-Anderson J, Farley E, Goddard P, Heintz R, Holladay B, Horn J, Johnson S, Lauth B, Moulton L, Norcross B, Parker-Stetter S, Seigle J, Sformo T (2015) Fish communities across a spectrum of habitats in the Beaufort and Chukchi seas. Synthesis of Arctic Research (SOAR) Special issue. Prog Oceanogr 136:115–132

Matarese AC, Kendall AW Jr, Blood DM, Vinter BM (1989) Laboratory guide to early life history stages of Northeast Pacific fishes. NOAA Technical Report NMFS, p 80

Matarese AC, Blood DM, Busby MS (2013) Guide to the identification of larvae and early juvenile pricklebacks (Perciformes: Zoarcoidei: Stichaeidae) in the northeastern Pacific Ocean and Bering Sea. NOAA Professional Paper 15, p 96

McCusker MR, Denti D, Van Guelpen L, Kenchington E, Bentzen P (2013) Barcoding Atlantic Canada's commonly encountered marine fishes. Mol Ecol Res 13:177–188

Mecklenburg CW, Steinke D (2015) Ichthyofaunal baselines in the Pacific Arctic region and RUSALCA study area. Oceanography 28:158–189

Mecklenburg CW, Mecklenburg TA, Thorsteinson LK (2002) Fishes of Alaska. American Fisheries Society, Bethesda, p 1037

Mecklenburg CW, Møller PR, Steinke D (2011) Biodiversity of Arctic marine fishes: taxonomy and zoogeography. Marine Biodivers 41:109–140

Mecklenburg CW, Byrkjedal I, Christiansen JS, Karamushko OV, Lynghammar A, Møller PR (2013) List of marine fishes of the Arctic region annotated with common names and zoogeographic characterizations. Conservation of Arctic Flora and Fauna, Akureyri. doi:10.13140/RG.2.1.2761.4962

Moser HG (1981) Morphological and functional aspects of marine fish larvae. In: Lasker R (ed) Marine fish larvae. University of Washington Press, Seattle, pp 90–131

Nelson JS (2006) Fishes of the World, 4th edn. Wiley, New York, xix+601 p

Norcross BL, Holladay BA, Busby MS, Mier KL (2010) Demersal and larval fish assemblages in the Chukchi Sea. Deep-Sea Res II 57:57–70

Nye JA, Link JS, Hare JA, Overholtz WJ (2009) Changing spatial distribution of fish stocks in relation to climate and population size on the Northeastern United States continental shelf. Mar Ecol Prog Ser 393:111–129

Orr JW, Matarese AC (2000) Revision of the genus *Lepidopsetta* Gill, 1862 (Teleostei: Pleuronectidae) based on larval and adult morphology, with a description of a new species from the North Pacific Ocean and Bering Sea. Fishery Bull US 98:539–582

Page LM, Espinoza-Pérez H, Findley LT, Gilbert CR, Lea RN, Mandrak NE, Mayden RL, Nelson JS (2013) Common and Scientific Names of Fishes from the United States, Canada, and Mexico, 7th edn. Am Fish Soc, Bethesda, p 384

Pertseva-Ostroumova TA (1961) The reproduction and development of far-eastern flounders. Tr Inst Okeanol Akad Nauk SSSR, p 484

Pietsch TW, Orr JW (2015) Fishes of the Salish Sea: a compilation and distributional analysis. NOAA Professional Paper NMFS 18, p 106

Posgay JA, Marak RR (1980) The MARMAP bongo zooplankton samplers. J Northwest Atl Fish Sci 1:91–99

Potthoff T (1984) Clearing and staining techniques In: Moser HG et al. (eds.) Ontogeny and systematics of fishes. Am Soc Ichthyol Herpetol Special Publ 1, Allen Press, Lawrence, pp 35–36

Roje DM (2010) Incorporating molecular phylogenetics with larval morphology while mitigating the effects of substitution saturation on phylogeny estimation: a new hypothesis of relationships for the flatfish family Pleuronectidae (Percomorpha: Pleuronectiformes). Mol Phylogenet Evol 56:586–600

Sheiko BA, Fedorov VV (2000) Chapter 1. Class Cephalaspidomorphi—Lampreys. Class Chondrichthyes—Cartilaginous fishes. Class Holocephali—Chimaeras. Class Osteichthyes—Bony fishes. p 7–69 in Katalog pozvonochnykh Kamchatki i sopredel'nykh morskikh akvatoriy [Catalog of vertebrates of Kamchatka and adjacent waters]. Kamchatsky Pechatny Dvor

Tabery MA, Chambers TJ, Gooda TP, Smith BA (1977) A multipurpose epibenthic sampler for fish eggs, larvae, juveniles and adults. Texas Instruments Inc, Ecological Services, Buchanan

Taranetz AJ (1937) Handbook for identification of fishes of Soviet Far-East and adjacent waters. Bull Pac Sci Fish Inst 11:1–200 (In Russian)

Wilderbuer TK, Nichol DG, Ianelli J (2015) Assessment of the yellowfin sole stock in the Bering Sea and Aleutian Islands. North Pacific Fisheries Management Council BASI SAFE, pp 733–820